J|A|C|S
ARTICLES
Published on Web 05/21/2005

Mercury Binding Sites in Thiol-Functionalized Mesostructured Silica

Simon J. L. Billinge,*,† Emily J. McKimmy,‡ Mouath Shatnawi,† HyunJeong Kim,† Valeri Petkov,§ Didier Wermeille,⊥ and Thomas J. Pinnavaia*,‡

Contribution from the Department of Physics and Astronomy, Michigan State University, East Lansing, Michigan 48824, Department of Chemistry, Michigan State University, East Lansing, Michigan 48824, Department of Physics, Central Michigan University, Mount Pleasant, Michigan 48859, and Department of Physics and Astronomy, Iowa State University, Ames, Iowa 50011

Received February 2, 2005; E-mail: pinnavaia@chemistry.msu.edu

Abstract: Thiol-functionalized mesostructured silica with anhydrous compositions of $(SiO_2)_{1-x}(LSiO_{1.5})_x$, where L is a mercaptopropyl group and x is the fraction of functionalized framework silicon centers, are effective trapping agents for the removal of mercuric(II) ions from water. In the present work, we investigate the mercury-binding mechanism for representative thiol-functionalized mesostructures by atomic pair distribution function (PDF) analysis of synchrotron X-ray powder diffraction data and by Raman spectroscopy. The mesostructures with wormhole framework structures and compositions corresponding to $x = 0.30$ and 0.50 were prepared by direct assembly methods in the presence of a structure-directing amine porogen. PDF analyses of five mercury-loaded compositions with Hg/S ratios of 0.50−1.30 provided evidence for the bridging of thiolate sulfur atoms to two metal ion centers and the formation of chain structures on the pore surfaces. We find no evidence for Hg−O bonds and can rule out oxygen coordination of the mercury at greater than the 10% level. The relative intensities of the PDF peaks corresponding to Hg−S and Hg−Hg atomic pairs indicate that the mercury centers cluster on the functionalized surfaces by virtue of thiolate bridging, regardless of the overall mercury loading. However, the Raman results indicate that the complexation of mercury centers by thiolate depends on the mercury loading. At low mercury loadings (Hg/S $\leq$ 0.5), the dominant species is an electrically neutral complex in which mercury most likely is tetrahedrally coordinated to bridging thiolate ligands, as in $Hg(SBu^t)_2$. At higher loadings (Hg/S 1.0−1.3), mercury complex cations predominate, as evidenced by the presence of charge-balancing anions (nitrate) on the surface. This cationic form of bound mercury is assigned a linear coordination to two bridging thiolate ligands.

Introduction

Mercury, a toxin known to cause neurological impairment in humans, is of great environmental concern. One promising technique for achieving the removal of low levels of mercuric ions from groundwater is to trap them using complexing ligands (e.g., thiols) that are covalently linked to a high surface area support.[1] Accordingly, various forms of thiol-functionalized mesostructured silica have been examined as candidates for mercury remediation.[2−5] These trapping agents offer very high surface areas, well-defined pore sizes, and high thiol group loadings with up to 50% of the framework silicon centers being functionalized.[6,7] Linking the organic moiety to the mesostructure can be accomplished either by grafting a thiol-functional silane reagent to the surface silanol groups of the mesostructure[2−4] or by the direct incorporation of the organosilyl group into the framework walls during synthesis.[6−8] The direct assembly pathway is generally preferred over grafting, in part, because the trapping agent can be prepared in a one-pot process, as opposed to the multiple processing steps involved in grafting. Also, the direct assembly process provides a higher concentration and a more uniform distribution of organo groups on the surface of the support.[8]

Recently, an XAS study[9] was reported for mercury bound to the thiol groups of a mercaptopropyl-functionalized silica mesostructure with a wormhole framework structure, denoted MP-HMS. The EXAFS data indicated the presence of Hg−S

† Department of Physics and Astronomy, Michigan State University.
‡ Department of Chemistry, Michigan State University.
§ Central Michigan University.
⊥ Iowa State University.

(1) U.S. EPA. *Capsule Report: Aqueous Mercury Treatment*; Office of Research and Development, 1997.
(2) Mercier, L.; Pinnavaia, T. J. *Adv. Mater. (Weinheim, Germany)* **1997**, *9*, 500−503.
(3) Feng, X.; Fryxell, G. E.; Wang, L. Q.; Kim, A. Y.; Liu, J.; Kemner, K. M. *Science (Washington, D. C.)* **1997**, *276*, 923−926.
(4) Liu, A. M.; Hidajat, K.; Kawi, S.; Zhao, D. Y. *Chem. Commun. (Cambridge)* **2000**, 1145−1146.
(5) Lim, M. H.; Blanford, C. F.; Stein, A. *Chem. Mater.* **1998**, *10*, 467−470.
(6) Mori, Y.; Pinnavaia, T. J. *Chem. Mater.* **2001**, *13*, 2173-2178.
(7) Shah, J.; Kim, S.-S.; Pinnavaia, T. J. *Chem. Commun. (Cambridge)* **2004**, 572−573.
(8) Walcarius, A.; Etienne, M.; Lebeau, B. *Chem. Mater.* **2003**, *15*, 2161−2173.
(9) Chen, C.-C.; McKimmy, E. J.; Pinnavaia, T. J.; Hayes, K. F. *Environ. Sci. Technol.* **2004**, *38*, 4758−4762.

10.1021/ja0506859 CCC: $30.25

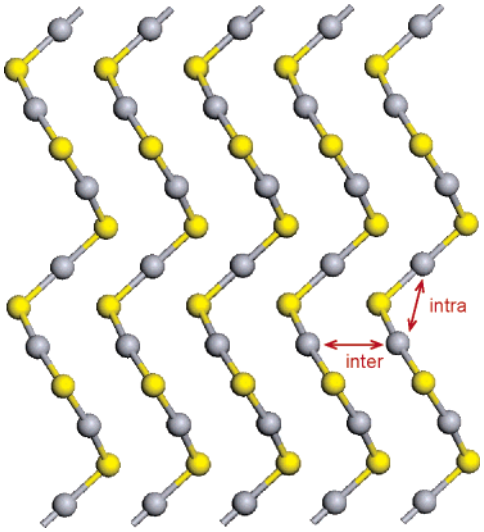

Figure 1. Cinnabar (HgS) structure (yellow = S, gray = Hg).

bonds, as expected, as well as an equivalent population of Hg−O bonds. These findings favored a predominance of S−Hg−O over S−Hg−S linkages for Hg/S ratios ≤ 1.0. A shortcoming of EXAFS is that structural information falls off quickly with increasing distance from the probe element, and it is difficult to learn about the positions of atoms beyond the nearest neighbor coordination shell. This limitation is especially acute for Hg L3 spectra.[10−14] In the earlier XAS work[9] it was not possible to differentiate between localized and extended networks or to establish the precise nature of the Hg binding. For thiol-functionalized mesostructures in which 30% to 50% of the silicon centers are functionalized[3,15] and available for binding to mercury, it is plausible that extended −Hg−S− chains could form within the pores through the bridging of thiolate ligands to two mercury centers. Such chain structures are found for the HgS structure, as illustrated in Figure 1.

The presence of bridging thiolate centers would be verified by observing a mercury−mercury contact similar to the intrachain Hg−Hg distance in HgS. If extended chain structures formed, it would be possible to observe interchain Hg−Hg distances. However, the limitations of the XAS technique, particularly when applied to mercury, preclude the detection of chain structures.

Another local structural technique that can provide information complementary to EXAFS is the atomic pair distribution function (PDF) analysis of X-ray powder diffraction data. This is a diffraction technique, used to study amorphous materials[16] and, more recently, successfully applied to nanocrystalline and crystalline materials.[17] The technique does not presume periodicity and can be applied to disordered materials. It yields high-quality information about structure on short and intermediate ranges and is a useful complement to the XAFS study.

Here we apply the PDF method, together with Raman spectroscopy, to study a series of thiol-functionalized mesoporous silicas with different mercaptopropyl content and Hg loading. Two types of wormhole framework structures with the anhydrous compositions $(SiO_2)_{1-x}(LSiO_{1.5})_x$, where L is the mercaptopropyl group, are prepared by direct assembly methods. The MP-HMS series of trapping agents made use of tetraethyl orthosilicate (TEOS) as the source of SiO_4 units.[6,18] The MP-MSU-SA compositions are made from sodium silicate as the SiO_4 source.[7] For both families of materials, mercaptopropyltrimethoxysilane was the precursor for the $LSiO_3$ units in the framework and dodecylamine is the structure-directing porogen.

We find clear evidence for the presence of bridging sulfur centers on the pore surfaces, analogous to the bridging sulfur centers in cinnabar and mercuric alkylthiolates. Also, in contrast to the XAS result for these trapping agents,[9] we see no evidence for Hg−O bonds and can certainly rule out oxygen coordination of the mercury at greater than the 10% level. A revised model is proposed for Hg binding in which S binds to two Hg neighbors and each mercury is bound to at least two sulfur centers, regardless of the mercury loading on the surface.

Experimental Section

Mesostructure Synthesis. Using both tetraethyl orthosilicate (TEOS) and sodium silicate as the silica source, we prepared mesostructured compositions with wormhole framework structures and anhydrous compositions of $(SiO_2)_{1-x}(LSiO_{1.5})_x$, where L is mercaptopropyl and x is the fraction of framework silicon centers that have been functionalized. Mesostructures assembled from tetraethyl orthosilicate (TEOS) were denoted MP-HMS, and those prepared from sodium silicate were denoted MP-MSU-SA. For both classes of materials, dodecylamine (DDA) was used as the structure-directing porogen and mercaptopropyltrimethoxysilane (MPTMS) was the source of the organosilicon centers.

The MP-HMS compositions were assembled at 65 °C in accord with a previously reported method,[6] except that the order of addition of reagents differed, with water being the last reagent added to the reaction mixture 65 °C. The mixture then was aged in a reciprocal water bath shaker at 65 °C for 36 h. Finally, the solution was filtered and the precipitate collected, air-dried, and subjected to Soxhlet extraction with ethanol to remove the surfactant. The overall molar stoichiometry employed was $(1-x)$ TEOS:x MPTMS:0.22 DDA:6.7 EtOH:160 H_2O.

The synthesis of MP-MSU-SA materials from sodium silicate was carried out at 45 °C by adding the sodium silicate reagent to a mixture containing MPTMS, surfactant, ethanol, and an amount of glacial acetic acid equivalent to the formal sodium hydroxide content of the sodium silicate.[7] After a reaction time of 20 h, the surfactant was extracted from the mesostructure with hot ethanol. The overall reaction stoichiometry was $(1-x)$ SiO_2:0.80$(1-x)$ NaOH:0.252 DDA:x MPTMS:0.80-$(1-x)$ acetic acid:3.4 EtOH:134 + 7.9$(1-x)$ H_2O.

Nitrogen adsorption measurements indicated the pore size of the micelle-templated mesostructures to be in the small mesopore to large micropore range (2.2 −1.5 nm), in accord with previously reported findings.[6]

Mercury Adsorption. A 500 mg quantity of $(SiO_2)_{1-x}(LSiO_{1.5})_x$ mesostructure with $x = 0.30$ or 0.50 was added to various volumes of a 1000 ppm $Hg(NO_3)_2$ to achieve specific Hg^{2+}/SH ratios. The suspensions were agitated for 48 (± 3) h, and the filtrate was analyzed

(10) Lennie, A. R.; Charnock, J. M.; Pattrick, R. A. D. *Chem. Geol.* **2003**, *199*, 199−207.
(11) Behra, P.; Bonnissel-Gissinger, P.; Alnot, M.; Revel, R.; Ehrhardt, J. J. *Langmuir* **2001**, *17*, 3970−3979.
(12) Bishop, D. B.; McCool, G. D.; Nelson, A. J.; Reynolds, J. G.; Baumann, T. F.; Fox, G. A.; DeWitt, J. G.; Andrews, J. C. *Microchem. J.* **2002**, *71*, 247−254.
(13) Collins, C. R.; Sherman, D. M.; Ragnarsdottir, K. V. *J. Colloid Interface Sci.* **1999**, *219*, 345−350.
(14) Hesterberg, D.; Chou, J. W.; Hutchison, K. J.; Sayers, D. E. *Environ. Sci. Technol.* **2001**, *35*, 2741−2745.
(15) Kemner, K. M.; Feng, X.; Liu, J.; Fryxell, G. E.; Wang, L. Q.; Kim, A. Y.; Gong, M.; Mattigod, S. *J. Synchrotron Radiat.* **1999**, *6*, 633−635.
(16) Klug, H. P.; Alexander, L. E. *X-Ray Diffraction Procedures for Polycrystalline and Amorphous Materials*, 2nd ed.; 1974.
(17) Billinge, S. J. L.; Kanatzidis, M. G. *Chem. Commun. (Cambridge)* **2004**, 749−760.
(18) Mercier, L.; Pinnavaia, T. J. *Adv. Mater.* **1997**, *9*, 500−503.

by colorimetric assay using diphenylthiocarbazone as an indicator.[19] The amount of mercury adsorbed by the mesostructure was determined by difference. Within experimental uncertainty, the uptake of mercury was quantitative up to a total Hg^{2+}/SH ratio of 1.00.

Raman spectra were recorded on a Bio-Rad FT Raman spectrometer equipped with a germanium CCD camera detector using 633 nm radiation from a HeNe laser for excitation and a resolution of 4 cm^{-1}. Laser power at the sample was estimated to be about 5mW, and the focused laser beam diameter was ~10 μm. A total of 200 scans were employed.

PDF Experiments. Powder samples were packed in flat plates with 1 mm thickness sealed with Kapton tape. The X-ray scattering experiments were conducted on the powder samples using X-rays of energy 76 keV (λ = 0.16248 Å) at the 6-IDD station of MUCAT at the Advanced Photon Source (APS) at Argonne National Laboratory. Diffraction data were collected using the recently developed rapid acquisition pair distribution function (RA-PDF) technique.[20] The data were collected using a circular image plate camera (mar345) with diameter of 345 mm, which was mounted orthogonal to the beam path. The sample holder to detector distance was 161.94 mm. Different collection times were used to obtain each data set. For the HgO and HgS reference compounds, five scans with a total collection time of about 4 min were needed. For the MP-HMS and MP-MSU-SA samples five to six scans were necessary with a longer collection time than the previous two standards. The collection time lasted from half an hour to an hour to get high-quality results for these mesostructured samples.

Raw data were combined and integrated using the software FIT2D[21] and then normalized with respect to the average monitor counts. The signal from an empty container was subtracted from the raw data, and various other corrections were made as described in detail in Egami and Billinge.[22] The total scattering structure function $S(Q)$ was obtained using the program PDFgetX2.[23] Finally, the PDF, $G(r)$, which gives the probability of finding an atom at a distance r away from another atom, was obtained by a Fourier transformation of $F(Q) = Q[S(Q) - 1]$ according to eq 1:

$$G(r) = \frac{2}{\pi}\int_0^\infty Q[S(Q) - 1]\sin(Qr)\,dQ \qquad (1)$$

where Q is the magnitude of the scattering vector.

The transformation of $F(Q)$ to $G(r)$ was carried out with a Q_{max} = 30.0 Å for both HgO and the HgS samples. For the MP-HMS and MP-MSU-SA samples the counting statistics were not as good as for the HgS and HgO, which forced us to truncate our $F(Q)$ at Q_{max} = 16.0 Å for all the mesoporous silicas.

Data from a MP-HMS sample with x = 0.50 with no adsorbed mercury was also collected, this time at the BESSRC-CAT 11-ID-C beam line at the APS. The sample was sealed in a capillary and measured with X-rays of energy 114.67 keV (λ = 0.1081 Å). Scattered radiation was collected with an intrinsic germanium detector coupled to a multichannel analyzer. Several runs were conducted and the resulting XRD patterns were averaged to improve the statistical accuracy and to reduce any systematic effect due to instabilities in the experimental setup. In this case the data processing was done with the help of the program RAD.[24]

Table 1. Mercury Content of $(SiO_2)_{1-x}(LSiO_{1.5})_x$ Mesostructures for PDF Analysis, L = Mercaptopropyl

sample	mesostructure designation	x	mmol Hg^{2+}/g	mmol Hg^{2+}/mmol SH
1	MP-HMS	0.50	2.52	0.50
2	MP-HMS	0.50	4.85	0.96
3	MP-HMS	0.50	6.33	1.30
4	MP-MSU-SA	0.30	2.99	0.92
5	MP-MSU-SA	0.50	4.16	0.91

Results and Discussion

PDF Studies. Representative mercaptopropyl-functionalized mesostructures with 3D wormhole framework structures and anhydrous compositions of $(SiO_2)_{1-x}(LSiO_{1.5})_x$, where L = mercaptopropyl, were prepared and equilibrated at ambient temperature with known amounts of aqueous mercuric nitrate. At the initial ambient pH of the mercuric ion solution (~2.3) the predominant solution species is Hg^{2+}(aq) and the minor species is $Hg(OH)^+$.[25] At equilibrium, the final pH of the solution was near neutral, so that any mercury remaining in the solution was mainly in the form of $Hg(OH)_2$. For the MP-HMS mesostructures assembled from tetraethyl orthosilicate, the fraction of framework silicon centers containing a covalently bound thiol group was held constant at x = 0.50 and the bound Hg^{2+} to total S ratio was varied from 0.50 to 1.30. The compositions assembled from sodium silicate, denoted MP-MSU-SA, had x = 0.30 or 0.50 and a bound Hg^{2+} to total S ratio of ~0.91. The compositions are summarized in Table 1.

The structure functions for the Hg-loaded mesostructures are shown in Figure 2a, and the resulting PDFs, $G(r)$, in given in Figure 2b. The curves are offset from each other for clarity. Features in $F(Q)$ are broad, indicating the disordered nature of these materials, and this is reflected in $G(r)$ as a rapid falloff in structural features with increasing r. Also shown for comparison is the $F(Q)$ and PDF of mercury-free bulk silica glass. The curves for the Hg-loaded mesostructures are similar in shape, but quite distinct from the bulk silica glass. The presence of the strongly scattering Hg center is clearly evident. In particular, strong peaks in $G(r)$ at 2.4 and 3.7 are evident in the Hg-loaded samples that are not present in the silica. The peak at 1.6, which is present in all of the samples, originates from the Si−O distance in the silica network, but the 2.4 and 3.7 peaks arise from the pairing of mercury with atomic neighbors.

As indicated by the definition of $G(r)$ in eq 1, the intensity of a peak in the PDF coming from the pair of atoms i and j is scaled by $n_iZ_in_jZ_j/\langle Z\rangle^2$, where Z_i is the atomic number and n_i the coordination number of the ith ion and $\langle Z\rangle$ is the compositionally averaged atomic number of the entire sample. Thus, as the Hg loading increases, $\langle Z\rangle$ increases and the Si−O peaks at r = 1.6 change in magnitude, even though they have the same origin in all the samples. The PDFs were rescaled in such a way that the Si−O peak in each sample has the same integrated intensity. This was accomplished not by average scattering intensity, but rather by rescaling of the silica volume using the assumption that the mesostructures have similar morphologies and approximately the same sample volume.

These are the same $G(r)$'s shown in Figure 2, except they have been rescaled so the Si−O silica peaks at r = 1.6 have

(19) Zamzow, M. J. E., Eichbaum, B. R.; Sandgren, K. R.; Shanks, D. E. *Sep. Sci. Technol.* **1990**, *25*, 1555−1569.
(20) Chupas, P. J.; Qiu, X.; Hanson, J. C.; Lee, P. L.; Grey, C. P.; Billinge, S. J. L. *J. Appl. Crystallogr.* **2003**, *36*, 1342−1347.
(21) Hammersley, A. P.; S. O. S.; Hanfland, M.; Hauserman, D. *High-Pressure Res.* **1996**, *14*, 235.
(22) Egami, T.; Billinge, S. J. L. *Underneath the Bragg Peaks: Structural analysis of complex materials*; Pergamon Press Elsevier: Oxford, England, 2003.
(23) Qiu, X.; Thompson, J. W.; Billinge, S. J. L. *J. Appl. Crystallogr.* **2004**, *37*, 678.
(24) Petkov, V. *J. Appl. Crystallogr.* **1989**, *22*, 387−389.
(25) Baes, C. F., Jr.; Mesmer, R. E. *The Hydrolysis of Cations*; John Wiley & Sons: New York, 1976.

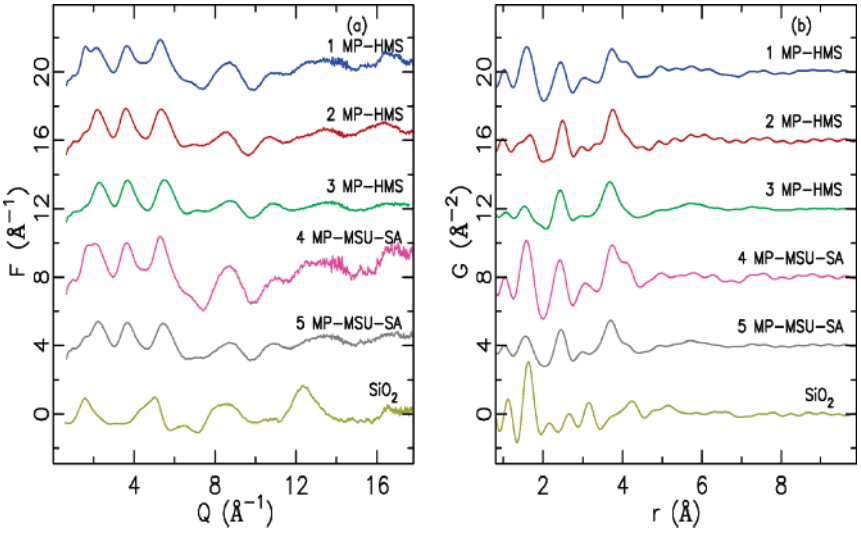

Figure 2. (a) Experimental $F(Q)$ and (b) the corresponding $G(r)$ for the mercury-loaded compositions of Table 1. Included for comparison are analogous data for bulk silica glass, labeled SiO_2, which does not contain mercury. The curves are offset for clarity.

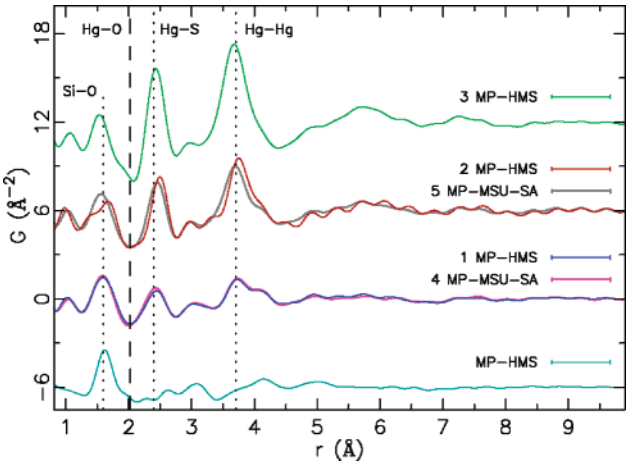

Figure 3. Rescaled PDF profiles for the Hg-loaded MP-HMS mesostructures.

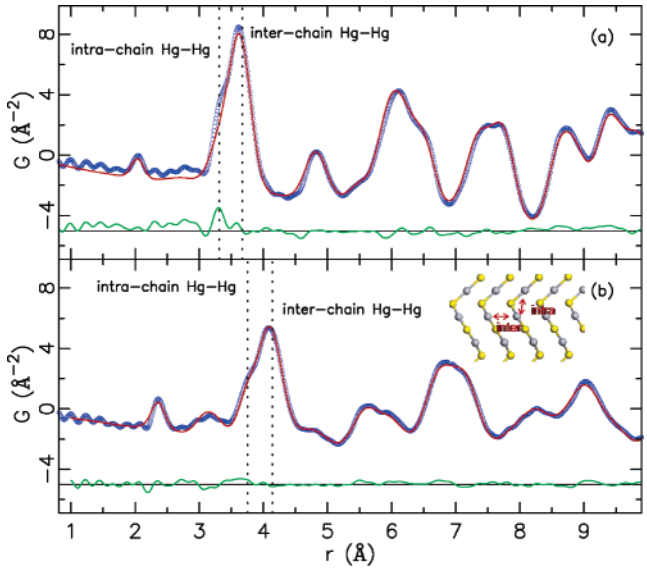

Figure 4. Experimental PDF (blue circles) and the PDF profiles calculated from the refined crystal structure (red line) for (a) HgO and (b) HgS reference compounds. The difference curves are represented by the offset green lines.

the same integrated area. Included for comparison is the PDF of the MP-HMS trapping agent ($x = 0.50$) without bound mercury.

The rescaled PDF profiles and the assignment of peaks in the profile are shown in Figure 3. Referring to Table 1, we see that samples **1** and **4** have similar Hg loadings and have the least adsorbed Hg, samples **2** and **5** have ∼50% more adsorbed Hg and are similar to each other in total Hg loading, and sample 3 has the highest Hg loading. It is evident from Figure 3 that the peaks at 2.4 and 3.7 follow this trend and arise principally from pairs of atoms involving Hg, more specifically, Hg−S and Hg−Hg pairs, respectively, as discussed more fully below. In the low-loaded samples **1** and **4** the 2.4 and 3.7 peaks are weak. They grow in the medium loadings of **2** and **5**, and they dominate the silica peaks in the heavily mercury loaded **3** composition. The broad bumps centered near 5.75 and 6.25 most likely originate from Hg pairs beyond the second nearest neighbor, but these Hg pairs are quite disordered.

To verify the peak assignments in the PDF profiles of the mercury-loaded mesostructures, we consider the isostructural reference compounds HgS[26] and HgO.[27] These show representative bonding environments of Hg^{2+} with S and O, respectively. The Hg prefers to have two neighbors arranged linearly with Hg−S bonds of 2.36 Å. The Hg−S−Hg bond angle is 104.73°, resulting in 1D zigzag −Hg−S−Hg−S− chains,[26] as represented in Figure 1. The situation is the same in HgO except that $r_{Hg-O} = 2.02$ Å and the Hg−O−Hg bond angle is 109.8°.[27] For comparison, we have measured the PDFs of these structures. They are shown in Figure 4 with the average crystal structure refined to the data using the real-space profile-fitting program PDFFIT[28] plotted on top. The experimental and calculated PDF profiles agree well, indicating that the RAPDF method clearly results in an accurate PDF. The refined values of the structural parameters from the fits of the experimental data are summarized in Table 2, along with the literature values.

An earlier XAS study[9] indicated the presence of a similar number of Hg−O as Hg−S bonds for Hg-loaded mesostructures

(26) Wyckoff, R. W. G. *Crystal Structures*; Interscience Publishers: Easton, PA, 1963; Vol. 1.
(27) Roth, W. L. *Acta Crystallogr.* **1956**, *9*, 277−280.
(28) Proffen, T.; Billinge, S. J. L. *J. Appl. Crystallogr.* **1999**, *32*, 572−575.

Table 2. Lattice Parameters Reported in the Literature and the Refined Values Obtained from the Experimental PDF Profiles for HgO and HgS[a]

HgO			HgS		
	literature value[27]	refined value		literature value[26]	refined value
a	3.311	3.3013	*a* = *b*	4.149	4.1289
b	5.526	5.5146	*c*	9.495	9.4591
c	3.526	3.5163	Hg (*x*/*a*)	0.720	0.7190
O (*z*/*c*)	0.17	0.157	S (*x*/*a*)	0.485	0.4913

[a]Included are the fractional coordinates for selected atomic positions.

equivalent to those studied in the present work. We thus seek a peak in the PDF of our samples at 2.02 that might originate from Hg−O. In the PDF of crystalline HgO, shown in Figure 4, the Hg−O peak is somewhat weak due to the weak scattering power of oxygen, but it is clearly apparent. However, there is no evidence for this peak in the data from the Hg-loaded mesoporous silicas (cf., Figures 2 and 3). Oxygen has half the number of electrons and, therefore, half the scattering power of sulfur. Therefore, if there were an equal number of Hg−S and Hg−O bonds, as suggested from the earlier XAS study, we would expect a Hg−O peak at 2.02 with an intensity roughly half as large as the Hg−S peak at 2.36. In fact, rather than a peak, a deep valley is evident at the expected Hg−O bond distance of 2.0 Å for all of the mesostructured samples (cf., Figures 2b and 3).

It is worth noting that the previously reported XAS studies of Hg binding to MP-HMS[9] mesostructures revealed the presence of only one significant RDF peak due to near-neighbor contacts. Well-crystallized cinnabar and meta-cinnabar also exhibited a single RDF peak corresponding to the inner coordination sphere of mercury only. The lack of outer sphere coordination information generally is unexpected for an XAS structure analysis. But in the case of mercury this result is not unusual, because several other reports of Hg L3 spectra for HgO, HgS, and other mercury-containing compounds[10−14] failed to provide next nearest neighbor distances for reasons that are yet unclear.

The earlier XAS study[9] indicated that 50% of mercury neighbors were oxygen. However, there is little or no evidence for a Hg−O peak at the expected position of $r = 2.02$ Å in Figure 3. We would like to quantify the maximum number of Hg−O neighbors consistent with our PDF data. The PDF that would be obtained if mercury were bonded to oxygen and sulfur with 50:50 probability as indicated in the XAS result[9] was simulated. The results are shown in Figure 5c. Mercury coordinated to oxygen at the 50% level is clearly inconsistent with the PDF data. To investigate this further, we simulated PDFs with 10% (Figure 5b) and 0% (Figure 5a) Hg−O neighbors. The best agreement is the model with no Hg−O bonds present, although we cannot rule out the presence of Hg−O bonds below the ∼10% level.

We next consider the Hg−Hg second-neighbor peak at 3.7. In composition **1** with a low Hg^{2+} loading, this peak is double-valued, as it overlaps peaks in the same region due to the Si−Si and O−O pairs from the silica framework (see the PDF profiles for the mercury-free bulk silica glass in Figure 2 and the MP-HMS mesostructure in Figure 3). In the more heavily loaded compositions 2 and 3, the Hg−Hg peak dominates and it is clear that it is peaked at 3.7. The high-*r* shoulder evident

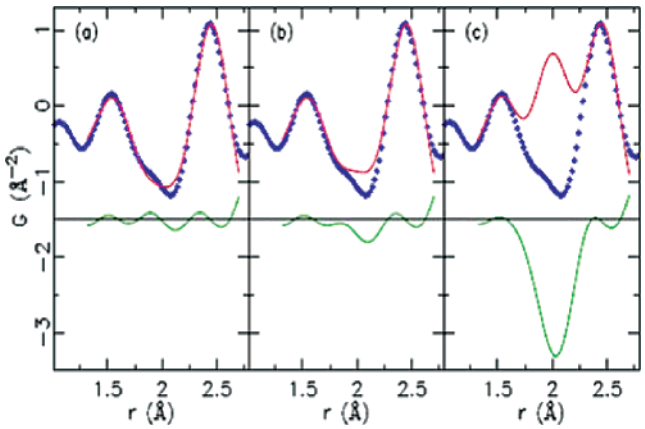

Figure 5. Calculated PDF profiles (red lines) assuming that (a) 0%, (b) 10%, and (c) 50% of the mercury centers in MP-HMS sample **3** ($x = 0.50$; Hg/S = 1.30) participated in Hg−O bond formation and the remaining mercury atoms bind to sulfur. The experimentally observed PDF profile for this mesostructure is shown by the blue circles. The difference curves are shown underneath in green. The Hg−O bond, if present, is expected to give rise to a peak at 2.02. The peaks at 1.6 and 2.36 are Si−O and Hg−S pairs, respectively.

Table 3. Atom Pair Distances for the HgS[26] and HgO[27] from the Models Reported in the Literature[a]

atom pair	distance (Å)
Hg−S (intrachain)	2.36
Hg−O (intrachain)	2.02
Hg−Hg (HgS intrachain)	3.75
Hg−Hg (HgS interchain)	4.14
Hg−Hg (HgO intrachain)	3.31
Hg−Hg (HgO interchain)	3.67

in the low-loaded samples is coming from the silica. The fact that this peak is strong, rather sharp, and well defined indicates that there are a significant number of Hg−Hg contacts in the pores and that they have a rather well-defined separation. This is expected if the thiolate sulfur atom bridges two mercury centers to form Hg−S−Hg linkages. Binding of thiolate sulfur to a single mercury center would lead to an irregular distribution of Hg and result in a rather broad distribution of Hg−Hg distances, in contrast to the well-defined peak that is observed. Bridging thiolate ligands, however, provide a well-defined Hg−Hg separation, because of the well-defined bond lengths and angles associated with covalent bonding. The relevant distances are available from the reference structures (Table 3 and Figure 4). The intrachain Hg−Hg contacts are 3.75 Å in HgS and 4.14 Å between the chains (cf., Figure 1). The 3.7 peak in the PDF corresponds closely to the expected Hg−Hg distance for a Hg−S−Hg linkage.

In agreement with the absence of Hg−O bonds, we also do not observe a strong Hg−Hg peak at 3.31 that would correspond to Hg−O−Hg linkages. Nor is there evidence of a strong interchain Hg−Hg peak at 4.14 that would correspond to zigzag chains of −Hg−S−Hg− packed alongside each other, as in the cinnabar structure. Because the thiolate sulfur centers are tethered to flexible hydrocarbon chains and encased inside nanoscale pores, it is not surprising that the surface −Hg−S−Hg− units do not order on the pore surfaces to give an interchain Hg−Hg contact.

Raman Studies. The Raman spectrum of the neat MP-HMS trapping agent in which 50% of the silicon centers contain mercaptopropyl functional groups (i.e., $x = 0.50$) is shown in

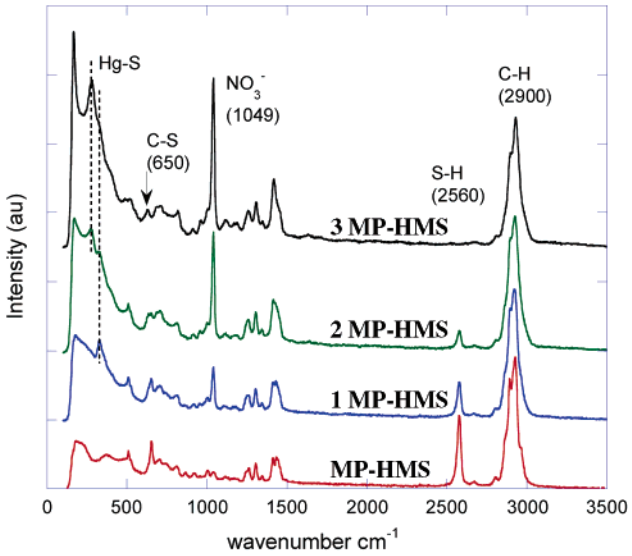

Figure 6. Raman spectra of thiol-functionalized $(SiO_2)_{1-x}(LSiO_{1.5})_x$ compositions ($x = 0.50$, L = mercaptopropyl) with a wormhole framework structure, denoted MP-HMS, and for the mercury-loaded compositions **1**, **2**, and **3** with Hg/S ratios of 0.50, 0.96, and 1.30, respectively. The spectra are offset on the *y*-axis for clarity.

Figure 6, along with mercury-loaded samples **1**, **2**, and **3** with Hg/S ratios of 0.50, 0.96, and 1.30, respectively.

The mercury-free trapping agent (MP-HMS) exhibits a well-expressed S−H stretch at 2560 cm^{-1}.[29,30] A weak band at 510 cm^{-1} assigned to a S−S stretch indicated the presence of a small amount of disulfide formation due to the air oxidation of adjacent thiol groups on the surface of the mesostructure.[30] The C−H stretching vibrations appear as strong bands near 2900 cm^{-1}, and the bands in the 1250−1500 cm^{-1} region correspond to C−H bending modes.[30]

The Raman-active Hg−S stretching vibration for mercury(II) thiolates in both the solid state and solution occur in the range 180−400 cm^{-1}.[31−34] The position of the stretching mode depends strongly on the coordination number of mercury to thiolate sulfur centers at a distance < 2.8 Å, as well as on the nature of the alkyl group.[31] Additionally, the stretching frequency of the C−S bond (600−725 cm^{-1}) is sensitive to the type of alkyl group bonded to the sulfur atom.[31,34] For mercury in linear 2-fold coordination to nonbridging methyl- and ethylthiolate in $Hg(SMe)_2$ and $Hg(SEt)_2$, the mode occurs at 297 and 394 cm^{-1}, respectively.[35] Mercury tetrahedrally coordinated to bulky *tert*-butylthiolate ligands in $Hg(SBu^t)_2$ exhibits a Hg−S Raman stretch at 188 cm^{-1}.[35] Thus, we assign the Raman band at 324 cm^{-1} for composition **1** with a Hg/S = 0.50 to a Hg−S stretching vibration. For compositions **2** and **3** with Hg/S = 0.96 and 1.3, respectively, this vibration is assigned to a band at 275 cm^{-1}.

The sharp band in the spectra of the mercury-loaded mesostructures at 1049 cm^{-1} is attributable to the presence of free (uncoordinated) nitrate ion. Free nitrate ion is known to exhibit a strong Raman-active band at 1050 cm^{-1}.[36] The assignment of this band to free nitrate in the MP-HMS compositions at Hg/S ratios of 0.50−1.30 is supported by the disappearance of the band upon washing the compositions with 0.1 M NaCl. Significantly, the relative intensity of the free nitrate band increases with increasing Hg/S ratio. Under conditions where the thiolate ligand is in large excess, e.g., at Hg/S = 0.10−0.30, no nitrate is associated with the bound mercury, as evidenced by the absence of the 1049 cm^{-1} band. Thus, at low mercury loadings the complexed form of the metal is electrically neutral. As the loading is increased (Hg/S ≥ 0.50), an increasing fraction of the trapped mercury adopts a cationic complex structure. At Hg/S = 1.3, all of the surface thiolate ligands are involved in complexation to mercury, as evidenced by the absence of a SH stretching band at 2560 cm^{-1} at this loading. The fact that the ratio of bound Hg/S to thiolate ligand can exceed a value of 1.0 suggests that some of the sulfur centers are triply bridging to mercury ions at high loadings.

We also note that with increasing mercury loading, a Raman band at 175 cm^{-1} appears. We are unclear as to the assignment of this peak. One possible explanation is that it indicates the presence of Hg_2^{2+}. The Hg−Hg stretching vibration of Hg_2^{2+} is reported to occur at 177 cm^{-1}.[37,38] The formation of Hg_2^{2+} has been reported to occur from photochemical reduction of Hg^{2+}.[39,40]

Conclusions

The PDF results, together with the Raman spectra, allow us to assign at least two binding modes for mercury(II) cations bound to $(SiO_2)_{1-x}(LSiO_{1.5})_x$ mesostructures, where L is a mercaptopropyl group. Under all mercury loadings conditions (i.e., Hg/S = 0.50−1.30) the thiolate groups bridge at least two mercury centers, leading to the a Hg−Hg contact in the PDF of 3.7 Å. At low mercury loadings, i.e., Hg/S ≤ 0.5, the predominant surface species is electrically neutral and not associated with a counteranion, as evidenced by the presence of little or no nitrate ion by Raman spectroscopy. For mercury binding under these conditions, we propose the presence of polymeric HgL_2 compositions in which the mercury adopts tetrahedral coordination to bridging thiolates as illustrated in Scheme 1. This structure is analogous to the bonding mode of mercury in $Hg(SBu^t)_2$.

Scheme 1

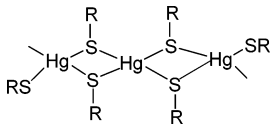

As the mercury loading is increased to a maximum value of 1.3, the predominant binding mode becomes cationic. The shift from an electrically neutral $Hg(SR)_2$ complex to a cationic complex with increasing Hg loading is supported by the increase

(29) Raso, S. W.; Clark, P. L.; Haase-Pettingell, C.; King, J.; Thomas, G. J., Jr. *J. Mol. Biol.* **2001**, *307*, 899−911.
(30) Kluth, G. J.; Carraro, C.; Maboudian, R. *Phys. Rev. B: Condens. Matter* **1999**, *59*, R10449−R10452.
(31) Hoffmann, G. G.; Brockner, W.; Steinfatt, I. *Inorg. Chem.* **2001**, *40*, 977−985.
(32) Biscarini, P. E. F. G. P. *J. Chem. Soc., Dalton Trans.* **1984**, 953−957.
(33) Biscarini, P.; Fusna, L.; Nivellini, G. *Spectrochim. Acta A* **1980**, *36A*, 593−600.
(34) Biscarini, P.; Fusina, L.; Nivellini, G. *J. Chem. Soc., Dalton Trans.* **1974**, 2140−2144.
(35) Casals, I.; Gonzalez-Duarte, P.; Sola, J.; Miravitlles, C.; Molins, E. *Polyhedron* **1988**, *7*, 2509−2514.
(36) Davis, A. R.; Irish, D. E. *Inorg. Chem.* **1968**, *7*, 1699−1704.
(37) Wickleder, M. S. *Z. Anorg. Chem.* **2002**, *628*, 1848−1852.
(38) Stammerich, H. T. T. S. *J. Mol. Struct.* **1967**, *1*, 55−60.
(39) Kim, C. S.; Rytuba, J. J.; Brown, G. E. *J. Colloid Interface Sci.* **2004**, *271*, 1−15.
(40) Kim, C. S.; Rytuba, J. J.; Brown, G. E. *J. Colloid Interface Sci.* **2004**, *270*, 9−20.

Scheme 2

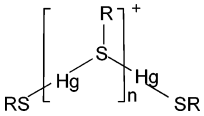

in the free nitrate ion in the Raman spectrum. The cationic species also is associated with the presence of bridging thiolate ligands, as supported by the continued presence of a Hg−Hg contact in the PDF. As shown in Scheme 2, we propose the predominant formation of a polymeric $Hg(SR)^+$ species at high mercury loadings in which the mercury centers adopt a linear 2-fold coordination to bridging thiolate ligands. This type of structure accounts for a Hg/S stoichiometry of 1.0. Because the observed Hg/S ratio can be as high as 1.3, it is possible that some of the thiolate ligands bridge to three mercury centers. Under no conditions do we find PDF evidence for binding of mercury to oxygen centers. Modeling studies of the expected PDF intensities for Hg−O contact pairs suggest that no more than 10% of the mercury centers are linked to oxygen centers.

Acknowledgment. This work was supported by NSF through grant CHE-0211029 and NIEHS grant ES04911. We made use of APS facilities, which are supported by the U.S. DOE, Office of Science, Office of Basic Energy Sciences, under Contract No. W-31-109-Eng-38. The MUCAT sector at the APS is supported by the U.S. DOE, Office of Science, under Contract No. W-7405-Eng-82.

JA0506859